Time-resolved fluorescence measurements for diffuse optical tomography using ultrafast time-correlated single photon counting

Yves Bérubé-Lauzière and Vincent Robichaud

Laboratoire TomOptUS, Département de génie électrique et de génie informatique
Université de Sherbrooke, 2500 boul. Université, Sherbrooke, Québec, J1K 2R1, Canada

ABSTRACT

We develop a novel approach to infer depth information about a small fluorophore-filled inclusion immersed in a scattering medium. It relies on time-resolved measurements of the time of flight distribution of emitted fluorescent photons after short pulse laser excitation. The approach uses a novel numerical constant fraction discrimination technique to assign a stable arrival time to the distribution's early photons. Our experimental results show a linear relationship between these arrival times and the position of the inclusion. This approach will serve as a useful technique in fluorescence diffuse optical tomography.

Keywords: Fluorescence, Diffuse Optical Tomography, Time-Resolved Measurements, Time-Domain, Time-Correlated Single Photon Counting, Numerical Constant-Fraction Discrimination, Time Point-Spread Functions

1. INTRODUCTION

Our motivation for the present work is to infer depth information about a small fluorophore-filled inclusion immersed in a scattering medium from time-resolved measurements of emitted fluorescence after short pulse laser excitation. The present work will serve in a fluorescence diffuse optical tomography (FDOT) scanner that we are developing for small animal *non-contact* molecular imaging. More precisely, our goal is to exploit the arrival time of early fluoresced photons to localize the inclusion with a time-of-flight (TOF) technique.

The rationale behind our approach is motivated by the following gedanken experiment: Imagine that a diffusing medium were not diffusing, that we had infinitely short laser pulses propagating as spherical waves, and that our fluorophore had an infinitely short lifetime, while emitting a spherical wave with a measurable amount of light when it fluoresces. The fluorophore can here be seen as a secondary source of light within the medium. Using spherical waves for describing light propagation provides a rough, but nevertheless useful, picture of how light pulses travel in a diffusing medium. In this thought experiment, after a laser pulse is injected into the medium, the time for the first fluorescent photons to be detected at a given position on the boundary of the medium is determined by 1) the time taken by the laser spherical wavefront to reach the inclusion, plus 2) the time for the fluoresced spherical wavefront to reach the detection position. Fig. 1 (a) illustrates the situation. By measuring the time between the injection of a laser pulse in the medium and the arrival of fluoresced photons at several locations around the medium, it is then possible to infer the position of the inclusion. This is a TOF technique, with several measurements around the medium being required to avoid ambiguity on the possible location of the inclusion (*i.e.* to break the degeneracy between symmetrical situations from the detector's point of view). Fig. 1 (b) illustrates this.

Correspondence should be sent to Y. B-L. at Yves.Berube-Lauziere@USherbrooke.ca

Advanced Photon Counting Techniques, edited by Wolfgang Becker, Proc. of SPIE
Vol. 6372, 637206, (2006) · 0277-786X/06/$15 · doi: 10.1117/12.685421

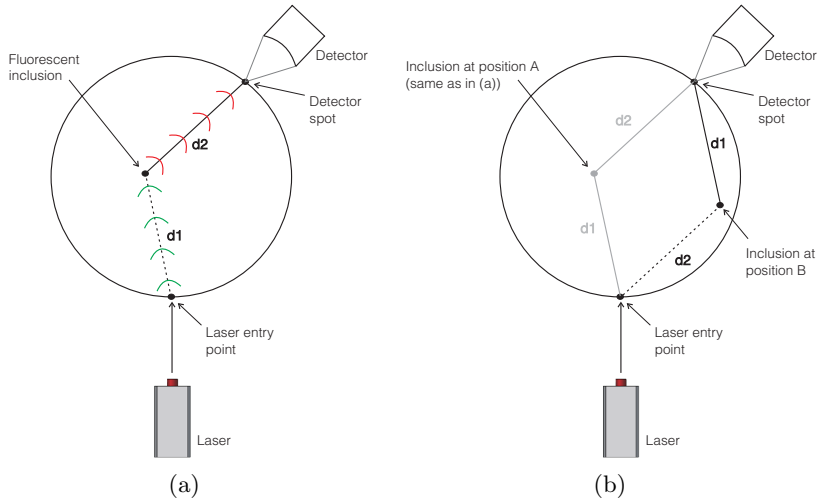

Figure 1. (a) Cross-sectionnal view of a cylindrical phantom used in the gedanken experiment. (b) Indistinguishable position (from the detector's temporal point of view) of the inclusion (in dark) from that shown in (a) (reproduced here in light gray). In both cases, the fluoresced light will reach the detector in the same time because the total path traveled (i.e. by the laser excitation pulse and the fluoresced light) is the same.

In reality, light pulses are broadened as they travel in diffusing media. Two types of photons can be distinguished: ballistic photons that do not suffer scattering events at all (which are not detectable[1] in thick ($>1cm$) biological tissues), and diffused photons whose time of flight distribution (time point-spread function (TPSF)) starts some delay after the time it takes for ballistic photons to propagate.[2] Consider the early arriving photons in real measurements of fluorescence TPSFs (FTPSFs), *i.e.* photons detected in the leading rising edge of an FTPSF. Being the fastest to reach the detector, 3 important facts can be said about them: 1) they must have resulted from the early laser photons that reached and excited the fluorophore, 2) they must have been emitted early by the fluorophore (*i.e.* in the early part of the fluorescence decay curve), and moreover, in both previous these processes, the photons must have followed a near ballistic path (*i.e.* be so-called "snake photons"). This brings us close to our gedanken experiment if we identify early photons with our spherical wavefronts.

Exploiting temporal information from time-resolved signals to infer the position of a fluorescent inclusion in a scattering medium has been first described by Feld, and coworkers.[3] Their approach uses the rising edge 50% point of the FTPSF maximum as the early photons arrival time. In further work,[4] the convolution theorem for Laplace transforms is exploited to devise a tomographic reconstruction algorithm from time-resolved data based on the diffusion approximation model for light propagation in scattering media. Their algorithm requires an optimal s value of the Laplace transform to be chosen. This choice is a trade-off between temporal (and consequently spatial) resolution (better at earlier times) and signal-to-noise ratio (SNR) (better at later times). However, no complete procedure on how to compute the optimal s is described. In a similar vein, Gallant et al. from ART have proposed to use the FTPSF maximum.[5] Their motivation was to determine the depth of fluorescent inclusions with ART's eXplore Optix ^{TM} system, a planar geometry time-resolved non-contact small animal imager.[6] Disadvantages of using the FTPSF maximum are: i) the FTPSF curve is relatively flat nearby the maximum, thus making the search for the maximum prone to errors due to noise, and ii) the maximum does

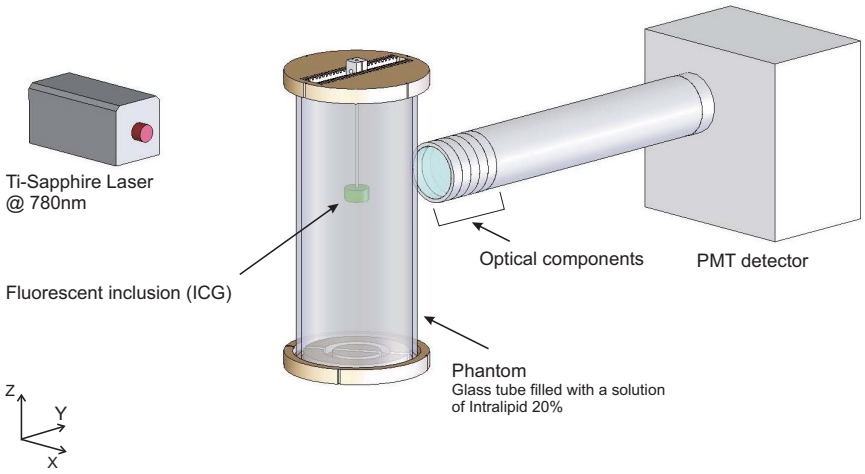

Figure 2. Schematic of the experimental setup showing the laser source, the phantom containing the fluorescent inclusion, the optical components (lens, attenuator, filters), and the PMT detector.

not convey information from the fastest detectable photons.

In this article, we assign a stable arrival time to early photons detected in the front edge of FTPSFs by way of a novel numerical constant fraction discrimination (NCFD) technique. Our experimental results show a clear linear relationship between these arrival times and the position of a fluorescent inclusion.

2. MATERIALS AND EXPERIMENTAL SETUP

2.1. Optical setup

A schematic of the experimental setup is shown in Fig. 2. A Tsunami laser (Spectra-Physics, Mountain View, CA, USA), is used (wavelength set to $780nm$, maximum output power = $750mW$, repetition rate = $80MHz$, pulse duration = $100fs$ FWHM). The optical power was attenuated by a neutral density absorptive filter to $47mW$ and directed to our phantom. Detection was made using a time correlated single photon counting (TCSPC) system (Becker&Hickl GmbH, Germany: SPC-134 and PMC-100 PMT). The PMT was cooled for reducing dark noise. The diffused light emitted from the phantom was first collected by a plano-convex lens (focal length = $25.4mm$) and then focussed onto the photocathode of the PMT by a plano-convex lens (focal length = $200mm$). With this configuration we image a ϕ= $1.25mm$ spot on the phantom onto the whole surface area of our PMT ($\phi = 10mm$). Between the two lenses, an optical attenuator is inserted to ensure that the intensity of detected light does not saturate or damage the PMT and that the photon flux is sufficiently small to prevent detection of multiple photons during each laser cycle (single photon counting limit).[7] Interference filters (Omega Filters, Brattleboro, VT, USA) were also inserted to attenuate as much as possible the laser wavelength.

2.2. Phantoms

We used a phantom to simulate tissue optical properties. It consisted of a 2 *inch* outer diameter glass tube (wall thickness = $1.5mm$, length = $12cm$) filled with a 48:1 (V/V) aqueous dilution of Intralipid 20% (Baxter). This suspension liquid yields a scattering coefficient of $\mu_s^{'} = 5cm^{-1}$.[8] In this scattering solution we inserted a

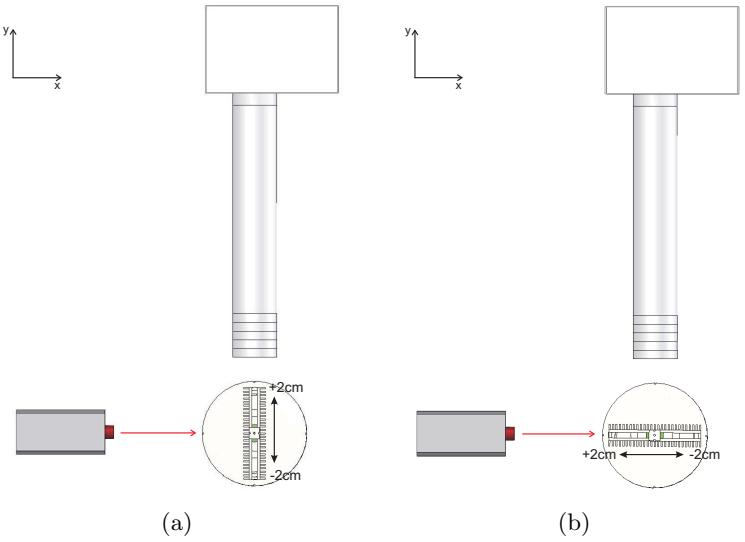

Figure 3. Top view of the setup. (a) Measurements taken by displacing the inclusion perpendicular to the laser beam axis. (b) Measurements taken by displacing the inclusion parallel to the laser beam axis.

fluorescent inclusion made with a glass tube (O.D. = $4mm$, wall thickness = $0.5mm$, length = $1cm$, caped at both ends) filled with indocyanine green (ICG) (Fisher Scientific), a NIR fluorescent agent (absorption peak @ $780nm$, emission peak @ $830nm$), at a concentration of $10\mu\text{Mol}/\ell$. The inclusion was attached at one end with a very thin nylon wire to allow us to fix it at a constant height along the z axis while being able to move it in the x-y plane.

2.3. Measurements

As shown in Fig. 3, we took measurements on the phantom at right angle with respect to the laser beam. The TCSPC collection time was 10 seconds. The cylinder surface was positioned a focal distance away from the collecting lens. The laser beam was adjusted at the same height as the inclusion and so that it hit the phantom at the center (Fig. 3). First, a background measurement (*i.e.* without an inclusion embedded in the medium) was made (Fig.4). As can be seen, we detected a small amount of light at the laser wavelength. Better optical filtering would have avoided this laser leak-through. We are currently working on more efficient optical filtering to avoid this. A first set of measurements was made by displacing the inclusion perpendicular to the axis of the laser beam (Fig. 3a) and a second set by displacing the inclusion parallel to the axis of the laser beam (Fig. 3b). The measurements consisted of a different position of the inclusion in the corresponding axis from -$2cm$ to +$2cm$ with a moving step of $2mm$. The raw data acquired with our TCSPC system consisted FTPSFs which combine the effect of the temporal broadening of the laser pulses within the medium, the fluorescence decay and the temporal broadening of the fluoresced light.

3. DATA PROCESSING

To eventually locate a fluorescent inclusion using information from early photons times of flight, we need to assign these photons a stable arrival time. In an ideal case, this would be the time at which the FTPSF starts

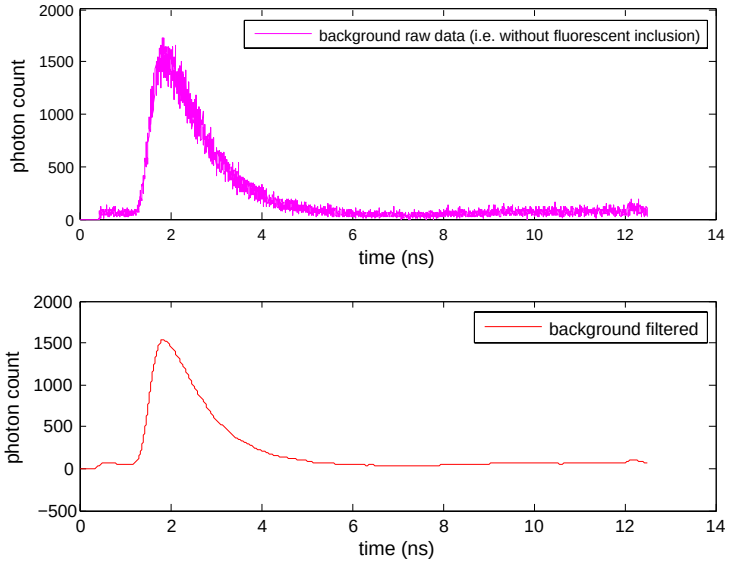

Figure 4. Plot of the signal obtained without a fluorescent inclusion embedded in the phantom. A small amount of laser leak-through is detected (max. number of photon counts around 1500)

rising. However, this is prone to noise in real measurements, since few photons are detected in that portion of the FTPSF. Using the rising edge of the FTPSF is a better alternative, but a leading edge discriminator cannot be used since FTPSFs vary in amplitude depending on the location of the inclusion. This is analogous to the difficulty met in the electronic detection of single photon PMT pulses in TCSPC systems.[9] We thus implemented a numerical constant fraction discriminator (NCFD) technique. The NCFD is designed to trigger on a certain optimum fraction of the FTPSF height. It results in a bipolar signal with a zero crossing which is independent of the pulse amplitude. *These zero crossings correspond to the arrival time we assign to the early fluoresced photons.* Fig. 5 illustrates the steps to achieve the NCFD. Each FTPSF and the background measurement were first smoothed with a digital Butterworth low-pass filter of order 2 and cutoff frequency at $3GHz$. Thereafter the smoothed background was subtracted from the smoothed FTPSF. This will be called the background subtracted filtered FTPSF (BSFTPSF). The BSFTPSF was then delayed (delay = $0.48ns$), inverted and attenuated by a fraction η of the original amplitude*. This was next added to the BSFTPSF. The bipolar signal obtained is finally analyzed to find its zero crossing.

4. RESULTS

The NCFD was applied to each FTPSF to find a relationship between the zero crossing and the position of the fluorescent inclusion in the scattering medium. As Fig. 6 exhibits, there is a nice quasi-linear relationship between the positions of the inclusion and the arrival times of early photons in the range from -1.2cm to +2cm for both perpendicular and parallel measurements. From -1.2cm to -2cm, the data do not to follow the same trend as the rest of the data. In fact, in this range, not enough fluoresced photons are collected for reliable data to be acquired. Fig. 7 (a) and (b) shows the degradation of the raw FTPSFs for perpendicular and parallel measurements as the

*η was set to 1.0 (no attenuation)

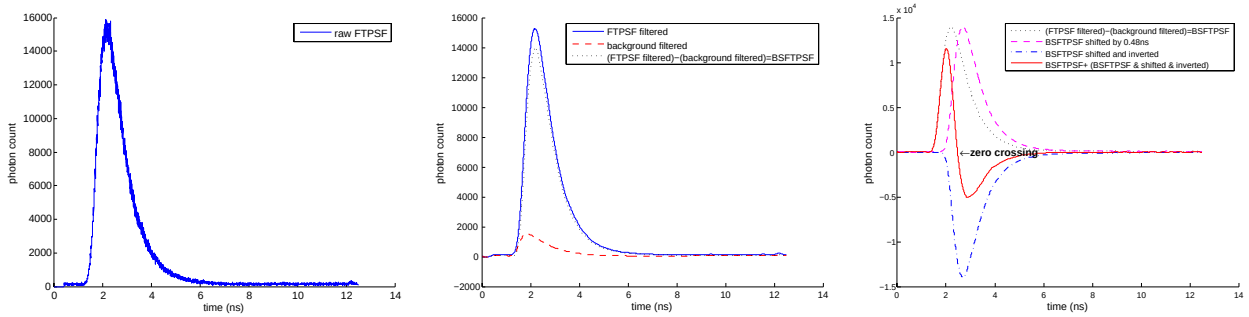

(a) (b) (c)

Figure 5. Steps to achieve our NCFD shown for raw data from a perpendicular measurement at position $+1.2cm$. (a) Raw data (FTPSF). (b) Filtered background signal subtracted from filtered FTPSF (BSFTPSF). (c) BSFTPSF added to a time delayed inverted version of the BSFTPSF resulting in a bipolar signal with a zero crossing.

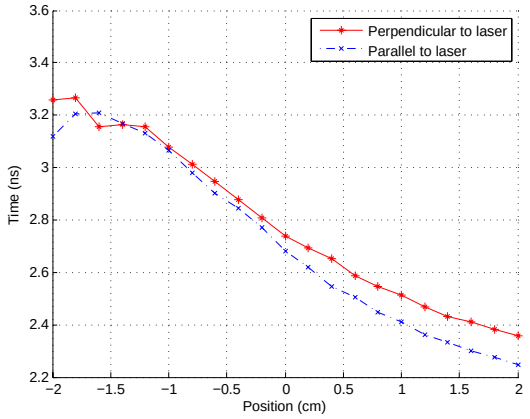

Figure 6. Graph showing the linear relationship between the positions of the fluorescent inclusion and the arrival time of early fluoresced photons as determined with our NCFD technique.

inclusion gets farther, and Fig. 7 (c) shows the NCFD result for a perpendicular measurement at -1.2cm. Notice the oscillations in the NCFD signal. We eliminate these cases by a simple thresholding technique: FTPSFs that do not contain enough photons are rejected (which is equivalent to say that the photon count rate was too low when they were acquired). For parallel measurements, this occurs when the inclusion is getting too far from the entry point of the laser into the phantom. Then not enough laser power reaches the inclusion to produce a reliable measurement at the detection spot on the phantom. In the case of perpendicular measurements, the inclusion is too far from the detection spot below -1.2cm. This shows clearly in Fig. 8 which serves to compare perpendicular measurements at (a) -1.2cm and (b) $+1.2cm$. Because of the symmetry of these positions with respect to the laser entry point, there is definitely enough laser light reaching the inclusion at -1.2cm. The reason is as follows: In perpendicular measurements, the path traveled by the laser light to reach the inclusion and the laser power exciting the inclusion are the same for symmetrical positions with respect to the center of the phantom ($0cm$), see Fig. 3 (a). The only parameter that influences the arrival time of the early fluoresced photons and the fluorescence intensity reaching the detection spot is the distance traveled from the inclusion to

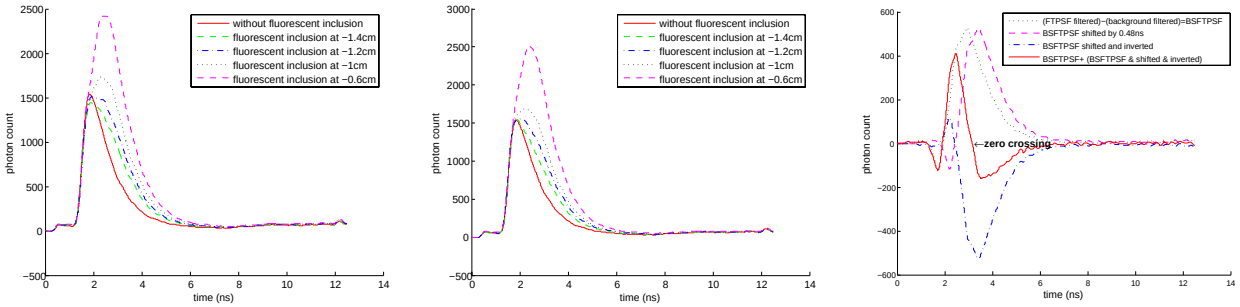

Figure 7. Filtered FTPSFs showing the degradation of the signal when the fluorescent inclusion is getting farther (a) from the detector in the case of perpendicular measurements, and (b) from the laser entry point in the case of parallel measurements. The farther the inclusion, the more alike is the signal to a background measurement. This illustrates the necessity for a background measurement. (c) shows the NCFD results for the -1.2cm measurement. Notice how the NCFD signal oscillates, being much more unstable as compared to FTPSFs containing more photons, see *e.g.* Fig. 5 (c).

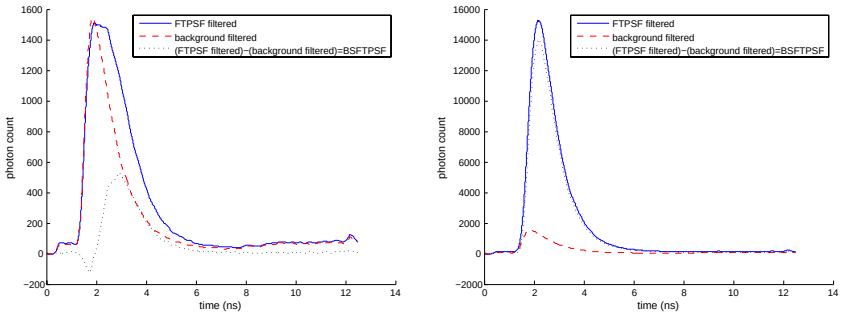

Figure 8. Comparing data at (a) -1.2cm and (b) +1.2cm for perpendicular measurements. Notice that the extent of the vertical scales are not the same in (a) and (b).

that spot. A similar reasoning is applicable to parallel measurements (see Fig. 3 (b)): For symmetrical positions of the fluorescent inclusion with respect to the center, the distance traveled by the fluoresced light to reach the detection spot is the same, but the path followed by the laser light that differs.

5. CONCLUSIONS AND FUTURE WORK

This work has focused on a stable NCFD technique to determine the arrival time of early photons in FTPSFs. It does not depend on the FTPSF amplitude, and is minimally prone to noise. Our measurements, made in a non-contact manner, and our experimental results show the usefulness of this technique in providing depth information from time-resolved signals. Indeed, a linear relationship between the arrival time and the depth of a fluorescent inclusion was demonstrated. These are very encouraging results towards deriving a time-of-flight based fluorescence diffuse optical tomography reconstruction algorithm for a non-contact small animal scanner we are developing. We were able to establish a simple criterion for discarding FTPSFs that do not provide

reliable arrival timing information. Our technique has the additionnal attractive feature that lower cost modern ultra-fast TCSPC technology can be used, instead of more expensive streak cameras, to determine precise timing information about early photons. This, even though TCSPC does not have the exquisite temporal resolution of streak cameras. In this respect, we nevertheless rely on the ability of modern TCSPC hardware to provide for high SNR and high sensitivity measurements. Our approach does not require obscure parameter selection. Only the delay and attenuation needed to implement the NCFD are required, parameters which have a simple sound physical interpretation. We are currently working on our next step, which is to use our NCFD technique to infer the 3D position of a fluorescent inclusion.

6. ACKNOWLEDGMENTS

Support from Spectra-Physics, Boston Electronics and Becker&Hickl in a Canada Foundation for Innovation (CFI) On-going New Opportunities Fund is gratefully aknowledged. This CFI grant has allowed the purchase of the the major equipements used in this work. Financial support from the Natural Sciences and Engineering Research Council of Canada (NSERC) (Discovery Grant and Research Tools and Instruments Grant) and the Universit de Sherbrooke (Fonds de dmarrage) has also made this research possible.

REFERENCES

1. e. G. Mueller et al., *Medical Optical Tomography: Functional Imaging and Monitoring*, SPIE Institutes for Advanced Optical Technologies, SPIE Press, 1993.
2. M. S. Patterson, B. Chance, and B. C. Wilson, "Time resolved reflectance and transmittance for the noninvasive measurement of tissue optical properties," *Appl. Opt.* **28**, pp. 2331–2336, 1989.
3. J. Wu, Y. Wang, L. Perelman, I. Itzkan, R. Dasari, and M. Feld, "Time-resolved multichannel imaging of fluorescent objects embedded in turbid media," *Opt. Lett.* **20**, pp. 489–491, 1995.
4. J. Wu, L. Perelman, R. Dasari, and M. Feld, "Fluorescence tomographic imaging in turbid media using early-arriving photons and laplace transforms," *Proc. Natl. Acad. Sci. USA* **94**, pp. 8783–8788, 1997.
5. P. Gallant, A. Belenkov, G. Ma, F. Lesage, Y. Wang, D. Hall, and L. McIntosh, "A quantitative time-domain optical imager for small animals in vivo fluorescence studies," in *OSA Conf. Biomed. Optics*, p. Paper WD2, 2004.
6. W. Long, Y. Bérubé-Lauzière, D. Hall, and L. McIntosh, "Method and apparatus for time resolved optical imaging of biological tissues as part of animals." US Pat. 6,992,762, January 2006.
7. F. E. W. Schmidt, M. E. Fry, E. M. C. Hillman, J. C. Hebden, and D. T. Delpy, "A 32-channel time-resolved instrument for medical optical tomography," *Rev. Sci. Instrum.* **71**, pp. 256–265, 2000.
8. J. Ripoll, M. Nieto-Vesperinas, R. Weissleder, and V. Ntziachristos, "Fast analytical approximation for arbitrary geometries in diffuse optical tomography," *Optics Letters* **27**, pp. 527–529, 2002.
9. W. Becker, *Advanced time-correlated single photon counting techniques*, Springer, New York, 2005 (1st Edition).